ISSN 1070-3284, Russian Journal of Coordination Chemistry, 2020, Vol. 46, No. 6, pp. 394–401. © Pleiades Publishing, Ltd., 2020.
Russian Text © The Author(s), 2020, published in Koordinatsionnaya Khimiya, 2020, Vol. 46, No. 6, pp. 349–356.

The authors congratulate Academician I.L. Eremenko with a 70th birthday

New Heteroligand Europium and Gadolinium Formate Triazole Dicarboxylates: Synthesis, Structures, and Luminescence Properties

Yu. A. Belousov[a, b, *], V. E. Goncharenko[a], A. M. Lunev[a], A. V. Sidoruk[a], S. I. Bezzubov[c], and I. V. Taidakov[b]

[a] *Moscow State University, Moscow, 119899 Russia*
[b] *Lebedev Physical Institute, Russian Academy of Sciences, Moscow, 119991 Russia*
[c] *Kurnakov Institute of General and Inorganic Chemistry, Russian Academy of Sciences, Moscow, 119991 Russia*
**e-mail: belousov@inorg.chem.msu.ru*

Received November 26, 2019; revised December 9, 2019; accepted December 24, 2019

Abstract—Complexes $\{(NMe_2H_2)[Ln(TDA)(HCOO)] \cdot 0.5H_2O\}$ are prepared by the solvothermal synthesis in a water–dimethylformamide (1 : 1) system from a mixture of 1,2,3-triazole-4,5-dicarboxylic acid (H_3TDA), NaOH, and $Ln(NO_3)_3$ (Ln = Eu, Gd). The crystal structure of the europium complex is determined by X-ray structure analysis (CIF file CCDC no. 1939689). This compound is shown to be the ionic metal-organic framework, where the cavities in the anionic structure of $[Eu(TDA)(HCOO)]^-$ are partially occupied by the dimethylammonium cations and water molecules. The study of the luminescence spectra of the gadolinium derivative gives the energy of the triplet level of the H_3TDA ligand (~25300 cm^{-1}), the value of which makes it possible to efficiently sensitize the luminescence of rare-earth metal ions, in particular, Eu^{3+}. The decay kinetics and the emission and excitation spectra of the heterometallic derivatives $\{(NMe_2H_2)[Gd_{1-x}Eu_x(TDA)(HCOO)] \cdot 0.5H_2O\}$ are studied. The dilution of europium with gadolinium results in a substantial decrease in the concentration quenching of the europium luminescence and an increase in the observed lifetimes of the excited state of Eu^{3+}.

Keywords: 1,2,3-triazoledicarboxylic acid, gadolinium, europium, luminescence, crystal structure, metal-organic frameworks

DOI: 10.1134/S1070328420050012

INTRODUCTION

The unique luminescence properties of rare-earth metal (REM) ions, first of all, europium, terbium, samarium, and dysprosium, can be used in the production of OLED devices [1–4] and sensor materials [5–8], for the protection of bank notes and securities [9], and for biovisualization [10–13]. Interest in the REM complexes with the structures of metal-organic frameworks (MOF) is related to the possibility of producing unique materials in which the sorption of guest molecules with the porous structure induces a luminescence sensor response [5, 14–18].

To obtain highly luminescing MOF based on REM ions, some rules should be fulfilled: the minimization of the number of OH, CH, and NH bonds in complex molecules favoring an efficient luminescence quenching of REM ions [19, 20]. Other mechanisms of REM ion quenching should also be suppressed, for example, concentration quenching. For this purpose, the dilution of the emitting REM ions with the heavy paramagnetic Gd^{3+} ion is applied [21]. In addition, the ligand should have a high energy of the triplet level (~20000 cm^{-1} for the europium complexes [22]) necessary for the sensitization of the REM ions. Some azolepolycarboxylic acids, for example, 1,2,3-triazole-4,5-dicarboxylic acid (H_3TDA) [5, 23], which is a very convenient "building" block for MOF formation, obey the indicated requirements. This is indicated by the possibility of forming single-, two-, and three-charged anions, as well as by exopolydenticity due to which one ligand molecule can simultaneously coordinate two [24], three [25], or four [26] metal ions. The deprotonated TDA^{3-} ion contains no CH, NH, and OH groups inducing multiphonon luminescence quenching.

Many crystal structures of 1,2,3-triazole-4,5-dicarboxylates of *d* metals, in particular, cobalt [27], copper [28], zinc [26], and cadmium [23, 24, 28], have been described to the present time. The complexes of

H_3TDA and structurally close ligand (benzimidazole-dicarboxylic acid) were reviewed [29].

The H_3TDA complexes with lanthanides are insufficiently presented in the literature. In particular, 3*d* MOF [23, 30], $[Ln(TDA)(H_2O)_3] \cdot H_2O$ structures, and 1*d* polymers [30, 31] were described. The terbium and europium derivatives were shown to exhibit an intensive ionic luminescence upon UV irradiation caused by the transitions inside the *f* shells of the REM. We proposed the heterometallic complex $[Tb_{0.9}Eu_{0.1}(TDA)]$ as a sensitive sensor for the determination of H_2O traces in heavy water D_2O and in aprotic organic solvents (dioxane and acetonitrile) [5].

The solvothermal synthesis of MOF was carried out in a water–dimethylformamide (DMF) mixture for the preparation of new H_3TDA complexes with REM. The formation of new compounds $\{(NMe_2H_2)[Ln(TDA)(HCOO)] \cdot 0.5H_2O\}$ (Ln = Eu (**I**), Gd (**II**)) was found. The formate anion and dimethylammonium cation are evidently formed due to DMF hydrolysis.

In this work, the crystal structure of the corresponding europium derivative and the luminescence properties of the europium, gadolinium, and mixed gadolinium–europium derivatives were studied.

EXPERIMENTAL

Commercially available reagents and solvents, as well as 1,2,3-benzotriazole (high-purity grade, Reakhim), were used. Europium and gadolinium nitrates were obtained by the dissolution of the corresponding oxides (99.999%, LANHIT, Russia) in concentrated nitric acid (reagent grade, XPC).

Synthesis of H_3TDA was carried out using a described procedure [32]. The reaction product was purified by double recrystallization from hot water, and the solution was refluxed with active carbon for 15 min for bleaching and filtered. The yield was 40%.

IR (ν, cm^{-1}): 3542 s, 2900–2400 m, 1720 m, 1585 m, 1534 w, 1395 w, 1295 m, 995 s. ^{13}C NMR (DMSO-d_6; δ, ppm): 161.5, 137.8.

For $C_4H_3N_3O_4$

Anal. calcd., %	C, 30.58	H, 1.92	N, 26.75
Found, %	C, 30.72	H, 2.00	N, 26.92

Synthesis of complexes I, II, and $\{(NMe_2H_2)[Eu_{1-x}Gd_x(TDA)(HCOO)] \cdot 0.5H_2O\}$ ($x = 0.1–0.9$). A Teflon container (10 mL) was loaded with DMF (3.00 mL), and H_3TDA (78.5 mg, 0.5 mmol), a 2 M solution of NaOH (500 μL), and a 0.2 M solution (2.5 mL) of $Eu(NO_3)_3$ (**I**) or $Gd(NO_3)_3$ (**II**) (or a mixture of these solutions in the corresponding volume ratio required for the heterometallic complexes) were added. The container was closed, placed in a steel autoclave, heated to 160°C (50°C/h), and kept at 160°C for 48 h. Then the container was cooled (2°C/h) to room temperature. The white precipitate formed was filtered under vacuum through a paper filter (blue band), washed with water (5 × 10 mL) and ethanol (2 × 10 mL), and dried in an evacuated desiccator over P_4O_{10} for 48 h.

Dimethylammonium [(1*H*-1,2,3-triazole-4,5-dicarboxylato(3-))(μ-formato)europiate(III)] · 0.5 hydrate (**I**): IR (ν, cm^{-1}): 3600–2800 s, 2730 vw, 2539 vw, 2436 vw, 1571 vs, 1422 m, 1369 m, 1272 m, 1157 vs, 1027 vw, 1014 vw, 859 s, 821 vs, 798 m, 783 m, 712 w, 530 s, 435 s). The yield was 85%.

For $C_7H_{10}N_4O_{6.5}Eu$

Anal. calcd., %	C, 20.70	H, 2.48	N, 13.79
Found, %:	C, 21.02	H, 2.50	N, 13.88

Dimethylammonium [(1*H*-1,2,3-triazole-4,5-dicarboxylato(3-))(μ-formato)gadolinato(III)] · 0.5 hydrate (**II**): IR (ν, cm^{-1}): 3600–2800 s, 2779 vw, 2543 vw, 443 vw, 1574 vs, 1425 m, 1370 m, 1276 m, 1159 vs, 1028 vw, 1015 w, 860 s, 822 vs, 798 s, 785 s, 713 w, 533 s, 438 s. The yield was 88%.

For $C_7H_{10}N_4O_{6.5}Gd$

Anal. calcd., %	C, 20.43	H, 2.45	N, 13.62
Found, %	C, 20.88	H, 2.52	N, 13.84

Elemental analysis was carried out using a Fision Instruments 1108 microanalyzer.

IR spectra were recorded on a FTIR Spectrum One Perkin-Elmer spectrometer in KBr pellets in a range of 400–4000 cm^{-1} with a resolution of 0.5 cm^{-1}. The photoluminescence spectra and lifetimes of the excited states of Eu^{3+} of the powdered samples were measured on a Varian Cary Eclipse spectrofluorimeter. All luminescence and excitation spectra were measured with a correction to instrumental functions. The measurements were performed in quartz cells with a diameter of 5 mm at room temperature. The error of lifetime measurements was 1%.

Thermal analysis was carried out on a NETZSCH STA 409 PC/PG instrument in air with a heating rate of 10°C/min. Powder diffraction patterns were detected using a Bruker D8 Advance diffractometer (CuK_α, λ = 1.5418 Å).

EDX analysis was conducted using a Leo Supra 50VP electron microscope equipped with an Oxford Instruments Xmax detector (voltage 15 kV, energy resolution 129 eV for the MnK_α line (5898.8 eV)). Statistical analysis of the EDX data for the determination of the Eu to Gd ratio in the complexes was performed using the ImageJ program package.

X-ray structure analysis. A single crystal of complex **I** was selected from the solvothermal synthe-

Table 1. Crystallographic data and experimental and structure refinement parameters for compound **I**

Formula	$[(CH_3)_2NH_2]^+[Eu(C_4N_3O_4)(HCO_2]^- \cdot 0.5H_2O$
FW	406.15
Crystal size, mm	0.10 × 0.12 × 0.34
Crystal system	Orthorhombic
Space group	$Pna2_1$
a, Å	12.7834(4)
b, Å	10.0323(3)
c, Å	8.8998(4)
V, Å^3	1141.37(7)
Z	4
ρ_{calc}, g/cm^3	2.364
μ, mm^{-1}	5.529
F(000)	780
Range of θ, deg	2.08–30.00
Index ranges	$-17 \le h \le 17$, $-14 \le k \le 14$, $-12 \le l \le 12$
Total number of reflections	22062
Independent reflections	3315 (R_{int} = 0.0486, R_{sigma} = 0.0303)
Completeness of data collection over θ, %	100
Number of variables/restraints	197/7
Goodness-of-fit for F^2	1.151
R_1 for $I > 2\sigma(I)$	0.0281
wR_2 (all data)	0.0568
$\Delta\rho_{max}/\Delta\rho_{min}$, e/Å^3	1.36/–1.51

sis products. The experimental data were collected on an Xcalibur Sapphire 3 automated four-circle diffractometer at 120 K (MoK_α radiation, λ = 0.71073 Å, graphite monochromator) in the κ scan mode. An absorption correction was applied by measurements of equivalent reflection intensities [33].

The structure was solved by a direct method and refined by full-matrix anisotropic least squares for F^2 for all non-hydrogen atoms [34]. The crystal of complex **I** was a racemic twin with the component ratio 0.84/0.16. In addition, the crystal structure was pseudosymmetric because of the arrangement of the heavy europium atoms corresponding approximately (by 87% according to checkCif) to the higher-symmetric group *Pnma*. The hydrogen atoms were placed in the calculated positions and refined using the riding model. The crystallographic data and experimental and structure refinement details are presented in Table 1.

The full tables of atomic coordinates, bond lengths, and bond angles were deposited with the Cambridge Crystallographic Data Centre (CIF file CCDC no. 1939689; deposit@ccdc.cam.ac.uk or http://www.ccdc.cam.ac.uk).

RESULTS AND DISCUSSION

The synthesis of the MOF based on triazoledicarboxylic acid and REM cations was carried out in water only [23, 30, 31]. The replacement of the solvent with a mixture of water and DMF made it possible to obtain new compounds **I** and **II**. The X-ray diffraction analysis (XRD) patterns for complexes **I** and **II**, the theoretical XRD pattern calculated from the crystal structure data, and the XRD patterns of a series of the heterometallic complexes are presented in Fig. 1. All compounds are isostructural, and their XRD patterns are well consistent with that calculated for the structure of compound **I**. An insignificant difference in relative intensities of individual reflections can be explained by the sample texture and the presence of a variable number of water molecules in the framework cavities.

Complex **I** was studied by differential thermal analysis (DTA) with the mass spectrometric detection of volatile products (Fig. 2). The water loss occurs in a range of 50–150°C (the loss of 0.5 water molecule per formula unit of complex **I** is 2.21% (calcd.) and 1.81% (exp.)). The complex is resistant to further heating, and its decomposition with subsequent oxidation to

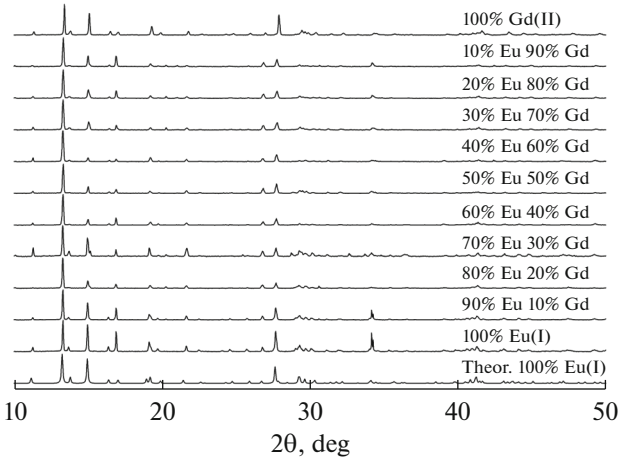

Fig. 1. Experimental XRD patterns of complex **II**, heterometallic series, and complex **I** and the theoretical XRD pattern calculated by the X-ray structure analysis data for complex **I** (see top-down).

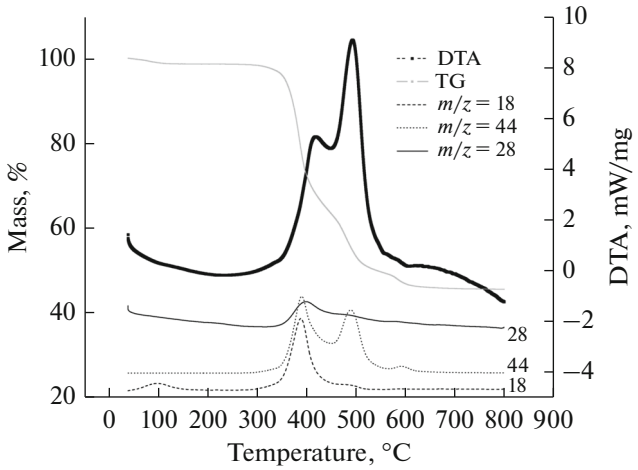

Fig. 2. Curves of the mass loss (TG) and DTA and the signals from the mass spectrometric detector of the thermal decomposition products for complex **I**.

Eu_2O_3, CO_2, H_2O, and N_2 begins only at the temperature higher than 330°C (mass loss: calcd. 56.5%, exp. 55.5%).

The crystal structure of complex **I** is built as a three-dimensional MOF formed by the anionic framework $[Eu(TDA)(HCOO)]^-$ (Fig. 3) and containing the $NMe_2H_2^+$ cations and water molecules in the cavities.

The europium cations are in the low-symmetry coordination environment (Fig. 4). The polyhedron can be described as a distorted two-capped trigonal prism with the bases N(1), O(1), O(5); N(3), O(2), and O(6) and vertices O(4) and O(3). Selected parameters for the crystal structure of complex **I** are presented in Table 2.

The average length of the Eu–O(TDA) bonds (2.4026 Å) appreciably exceeds the average O(HCOO)–Eu distance (2.3235 Å), indicating a stronger character of the latter. The Eu–N distances (av. 2.5615 Å) are longer than any Eu–O distance due to a higher electronegativity of oxygen.

All TDA^{3-} anions are equivalent, and each anion coordinates the europium cation by two donor atoms: by either two oxygen atoms (O(3) and O(2)), or the oxygen atom and nitrogen atom (O(1), N(1) and O(4), N(3)). The formate anions also act as bridging ligands linking two europium cations.

Owing to the use of the H_3TDA ligand, whose structure predetermines the framework polymeric character of the complexes formed by the ligand, the structure contains a system of channels with the maximum size ~7 × 7 Å. The view of the polymeric MOF structure along the *a* axis is shown in Fig. 2.

The dimethylammonium cations in the structure are disordered, and the shift of the nitrogen atoms between two positions is 1.255 Å. The disordering can be attributed to the fact that the size of the cavities in the framework substantially exceeds the sizes of the dimethylammonium cation.

Compound **I** irradiated with various wavelengths (254, 312, 365, and 405 nm) demonstrates the red-orange luminescence characteristic of the europium complexes. The irradiation of complex **II** with the short-wavelength UV light (254 nm) induces a weak blue-green luminescence of the ligand.

The phosphorescence spectrum of gadolinium complex **II** was detected to determine the energy of the triplet level of the H_3TDA ligand (Fig. 5). In order to determine the positions of the maxima, the spectrum was presented as a sum of three Gaussian components using the OriginPro 8 program package.

The spectrum exhibits three bands with the maxima at 396 (25300), 453 (22100), and 491 nm

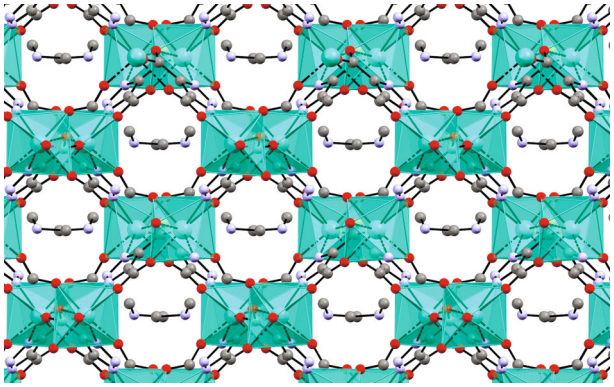

Fig. 3. Crystal structure of complex **I**. View along the crystallographic axis *a*. Hydrogen atoms are omitted.

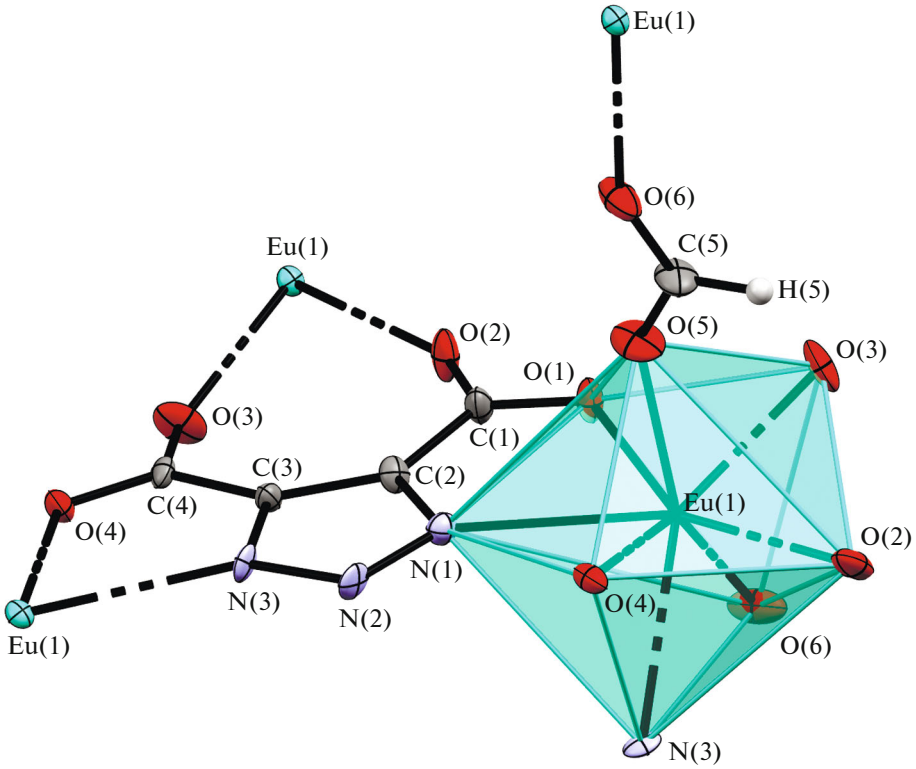

Fig. 4. Structure of the $[Eu(TDA)(HCOO)]^{-}$ anion according to the X-ray structure analysis data for complex **I**.

Table 2. Selected interatomic distances and bond angles in the structure of compound **I**

Bond	*d*, Å	Angle	ω, deg
Eu–O(1)	2.440(7)	O(3)EuN(3)	142.9(2)
Eu–O(2)	2.36(1)	O(5)EuO(6)	150.8(3)
Eu–O(3)	2.374(4)	O(1)EuO(2)	147.8(3)
Eu–O(4)	2.432(5)	O(4)EuO(6)	137.7(2)
Eu–O(5)(HCOO)	2.31(1)	O(5)EuN(1)	86.3(3)
Eu–O(6)(HCOO)	2.333(9)	O(3)EuN(3)	142.9(2)
Eu–O(av.)	2.375(1)	O(2)EuN(1)	148.3(3)
Eu–N(1)	2.572(6)	O(4)EuO(5)	71.3(3)
Eu–N(3)	2.554(6)	N(1)EuO(1)	63.8(2)
Eu–Eu(min)	6.8173(4)	N(1)EuO(6)	104.4(2)
Eu–Eu (bonded via μ_2HCOO^{-})	6.839(1)	O(1)EuN(3)	121.4(2)
Eu–N(4)($NMe_2H_2^{+}$)	4.20(1)	N(3)EuO(2)	80.5(3)
N4–O(1)	2.76(2)	O(2)EuO(5)	92.1(3)
N4–O(3)	3.03(1)	O(4)EuN(1)	72.7(2)
N4–O(7)(H_2O)	2.32(3)	N(3)EuN(1)	78.7(2)

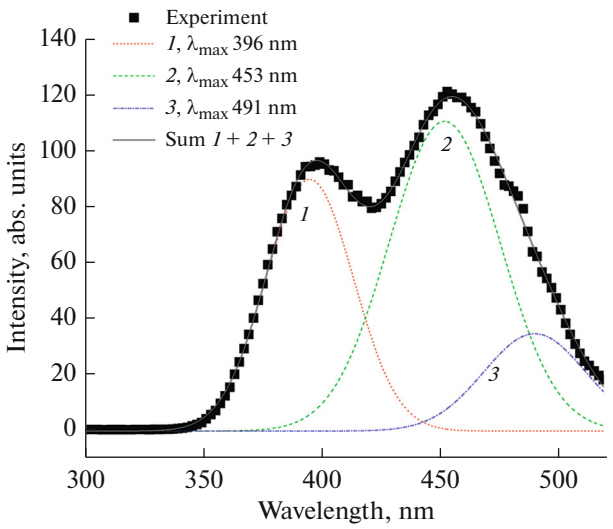

Fig. 5. Phosphorescence spectrum of complex **II** at room temperature (λ_{exc} = 254 nm) and its decomposition to Gaussians.

(20400 cm^{-1}). These bands should be assigned to the phosphorescence of the ligand. The observed lifetimes of the excited states (τ_{obs}) were determined for these bands as equal to 111, 126, and 120 μs (for wavelengths of 396, 453, and 491 nm, respectively). The energy of the first transition (25300 cm^{-1}) corresponds to the triplet level of the ligand. The energy gap between the triplet level of the ligand and resonance level of Eu^{3+} is very high and equal to ~8000 cm^{-1}. According to the Latva rule [22], this value should prevent an efficient transfer of the electron excitation energy. In spite of this fact, complex **I** luminesces upon UV irradiation, and the luminescence spectrum exhibits only the emission bands of europium. The latter is probably observed, because an efficient vibrational quenching is impossible in the studied system.

The emission and excitation spectra of complex **I** are presented in Fig. 6. The excitation spectrum exhibits both the broad band with a maximum at 254 nm and a number of narrow bands, the most intense of which has a maximum at 394 nm. The bands observed are assigned to the *f*–*f* transitions of the europium ion. Individual transitions were assigned to the spectral lines of europium on the basis of the literature data [35], and the assignment is shown in Fig. 6.

The photoluminescence spectrum of complex **I** has no broad line found for complex **II** and related to the intrinsic luminescence of the ligand. This indicates the completeness of the excitation energy transfer from the triplet level of the ligand to the resonance of europium $^5D_0$, i.e., the sensitization of the europium luminescence according to the antenna effect. The lifetime of the excited state of the Eu^{3+} ion determined from the decay kinetics of the $^5D_0$–$^7F_2$ transition was 645 μs. This is substantially higher than the lifetime in hydrate {[Eu(TDA)$(H_2O)_3$](H_2O)} [5], where τ_{obs} was 292 μs. The increase in τ_{obs} should be attributed to the suppression of the vibrational OH quenching after the water molecules were removed.

Nevertheless, the total luminescence intensity of complex **I** is low compared to that of other complexes. This can be related to various routes of nonradiative relaxation, in particular, concentration quenching. To check this assumption, we synthesized a series of the heterometallic complexes {(NMe_2H_2)[$Eu_{1-x}Gd_x$-(TDA)(HCOO)] · $0.5H_2O$)} (x = 0.1–0.9) under the conditions identical to those for the synthesis of compounds **I** and **II** in the pure state. The synthesized compounds are isostructural to individual complexes **I** and **II**, which was confirmed by the XRD analysis of the powder. The correspondence of the composition to that assumed by the synthesis was confirmed by the EDX method. The luminescence spectra detected for the samples of this series coincide completely with the luminescence spectra of complex **I** even at the Gd^{3+} content equal to 90%. The lifetimes τ_{obs} substantially

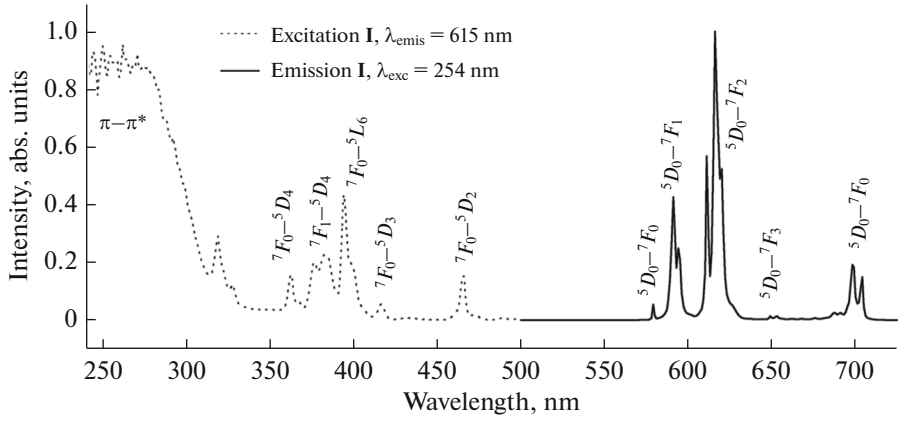

Fig. 6. Excitation and emission spectra of complex **I**.

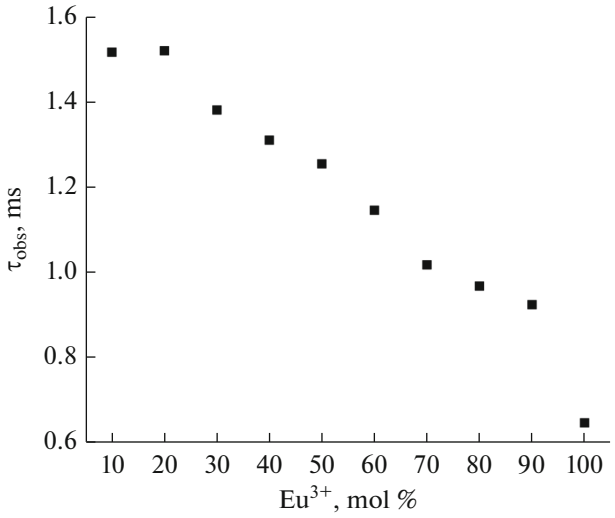

Fig. 7. Observed lifetime in the $\{(NMe_2H_2)[Eu_{1-x}Gd_x(TDA)(HCOO)] \cdot 0.5H_2O\}$ complexes vs. molar fraction of Eu^{3+}.

increasing with a decrease in the Eu^{3+} content (see Fig. 7) were also studied for these compounds. The maximum effect is achieved at the 20% molar fraction of europium, and then the intensity begins to decrease. This confirms that complex **I** contains a channel of nonradiative relaxation of the electron excitation energy of the Eu^{3+} ion related to the concentration quenching.

Thus, the replacement of water with a water–DMF mixture in the solvothermal synthesis of REM triazole dicarboxylates results in the formation of the heteroligand complexes containing the formate anion and dimethylammonium cation formed due to the hydrolysis of DMF along with the triazoledicarboxylate anion. The synthesized compounds contain no water or DMF in the nearest coordination sphere of the REM, which induces the luminescence of the europium complex undergoing no vibrational quenching. The method of europium dilution with gadolinium turned out to be successful for an additional increase in the lifetimes of the excited state, which decreases the concentration quenching and increases the observed lifetime of the excited state of europium by nearly 2.5 times.

ACKNOWLEDGMENTS

The X-ray studies were carried out on the equipment of the Center for Collective Use of the Kurnakov Institute of General and Inorganic Chemistry (Russian Academy of Sciences) in terms of the state task in the area of basic research of the Kurnakov Institute of General and Inorganic Chemistry (Russian Academy of Sciences).

FUNDING

This study was supported by the Russian Foundation for Basic Research, project no. 19-03-00263. The spectroscopic part of the work was supported by the Russian Science Foundation, project no. 19-13-00272.

CONFLICT OF INTEREST

The authors declare that they have no conflicts of interest.

REFERENCES

1. Korshunov, V.M., Ambrozevich, S.A., Taydakov, I.V., et al., *Dyes Pigments*, 2019, vol. 163, p. 291.
2. Taydakov, I.V., Akkuzina, A.A., Avetiso, R.I., et al., *Lumin.*, 2016, vol. 77, p. 31.
3. Girotto, E., Pereira, A., Arantes, C., et al., *Lumin.*, 2019, vol. 208, p. 57.
4. Panyushkin, V.T., Kapustina, A.A., Nikolayev, A.A., et al., *J. Appl. Spectr.*, 2019, vol. 85, p. 1133.
5. Gontcharenko, V.E., Lunev, A.M., Taydakov, I.V., et al., *IEEE Sens. J.*, 2019, vol. 19, p. 7365.
6. Turel, M., Čajlakovič, M., Austin, E., et al., *Sens. Actuators, B*, 2008, vol. 131, p. 247.
7. Almeida, N.A., Rodrigue, J., Silva, P., et al., *Sens. Actuators, B*, 2016, vol. 234, p. 137.
8. Sørensen, T.J., Kenwrigh, A.M., and Faulkner, S., *Chem. Sci.*, 2015, vol. 6, p. 2054.
9. Suyver, J.F. and Meijerink, A., *Chem. Weekblad.*, 2002, vol. 98, p. 12.
10. Yang, Y., Wang, P., Lu, L., et al., *Anal. Chem.*, 2018, vol. 90, p. 7946.
11. DaCosta, M.V., Doughan, S., Han, Y., and Krull, U.J., *Anal. Chim. Acta*, 2014, vol. 832, p. 1.
12. Eliseeva, S.V. and Bunzli, J.C.G., *Chem. Soc. Rev.*, 2010, vol. 39, p. 189.
13. Zairov, R.R., Shamsutdinova, N.A., Fattakhova, A.N., et al., *Izv. Akad. Nauk. Ser. Khim.*, 2016, vol. 5, p. 1325.
14. Luo, F. and Batten, S.R., *Dalton Trans.*, 2010, vol. 39, p. 4485.
15. Liu, H., Wang, H., Chu, T., et al., *J. Mat. Chem.*, 2014, vol. 2, p. 8683.
16. Hao, J.N. and Yan, B., *Chem. Commun.*, 2015, vol. 51, p. 7737.
17. Hao, J.N. and Yan, B., *J. Mat. Chem.*, 2014, vol. 2, p. 6758.
18. Ji, G., Liu, J., Gao, X., et al., *J. Mat. Chem. A*, 2017, vol. 5, p. 10200.
19. Clarkson, I., Dickins, R., and de Sousa, A., *J. Chem. Soc., Perkin Trans.*, 1999, vol. 2, p. 93.
20. Hemmilä, I., Mukkala, V.M., and Takalo, H., *J. Fluorescence*, 1995, vol. 5, p. 159.
21. Tobita, S., Arakawa, M., and Tanaka, I., *J. Phys. Chem.*, 1985, vol. 89, p. 5649.
22. Latva, M., Takal, H., Mukkala, V.M., et al., *J. Lumin.*, 1997, vol. 75, p. 149.
23. Chen, C.J., Gao, J.Y., Zhao, X., et al., *Z. Anorg. Allg. Chem.*, 2012, vol. 638, p. 2324.

24. Lin, L., Lin, Y.J., and Jin, G.X., *Appl. Organomet. Chem.*, 2019, vol. 33. e4759.
25. Zhou, X.H. and Chen, Q., *Cryst. Rep.*, 2017, vol. 62, p. 238.
26. Yuan, G., Shao, K.Z., Du, D.Y., et al., *Solid State Sci.*, 2011, vol. 13, p. 1083.
27. Li, L., Zou, J.Y., Gu, Z., et al., *Inorg. Chem. Commun.*, 2016, vol. 65, p. 59.
28. Zhao, T., Jing, X., Wang, J., et al., *Crystal Growth Des.*, 2012, vol. 12, p. 5456.
29. Zhang, S., Shi, W., and Cheng, P., *Coord. Chem. Rev.*, 2017, vol. 352, p. 108.
30. Zhang, X., Xu, N., Zhang, S.Y., et al., *RSC Adv.*, 2014, vol. 4, p. 40643.
31. Chen, C., Zhang, S.Y., Song, H.B., et al., *Inorg. Chim. Acta*, 2009, vol. 362, p. 2749.
32. Plaut, G.W.E., *J. Am. Chem. Soc.*, 1954, vol. 76, p. 5801.
33. Sheldrick, G.M., *Acta Crystallogr., Sect. A: Found. Crystallogr.*, 2008, vol. 64, p. 112.
34. Sheldrick G.M., *SADABS. Program for Scaling and Correction of Area Detector Data*, Göttingen: Univ. of Göttingen, 1997.
35. Binnemans, K., *Coord. Chem. Rev.*, 2015, vol. 295, p. 15.

Translated by E. Yablonskaya